RSC Advances

PAPER

View Article Online
View Journal | View Issue

Cite this: *RSC Adv.*, 2019, **9**, 14254

Transient bioelectrical devices inspired by a silkworm moth breaking out of its cocoon†

Qiaoyun Qi,[a] Yanru Li,[a] Wu Qiu,[a] Wenhai Zhang,[a] Chenyang Shi,[a] Chen Hou,[a] Wen Yan,[a] Jiani Huang,[a] Likun Yang,[a] Hao Wang,[a] Wenxi Guo,[a] Xiang Yang Liu [ba] and Naibo Lin *[a]

Transient devices have attracted extensive interest because they allow changes in physical form and device function under the control of external stimuli or related commands and have very broad application prospects for information security, biomedical care and the environment. Transient bioelectrical devices were fabricated inspired by a silkworm moth breaking out of its cocoon, which has shown many advantages, including the use of mild stimulation, biocompatible materials, a simple process, and a universal strategy. For the fabrication of the transient devices, heat-sensitive microspheres with a 9.3 mol L^{-1} LiBr solution in wax shells were prepared by microfluidic technology, which were then assembled into silk fibroin (SF) electronic materials/devices, such as SF conductive film, an LED circuit on SF film, and a Ag/SF film/Pt/SF film memristor. The contribution from the LiBr/wax microspheres to the transient time of the SF films upon exposure to heat was quantitatively investigated. This approach was applied to transiently dissolve a flexible Ag-nanowire resistance circuit line on a SF substrate. Moreover, memristors constructed with a functional layer of SF were destroyed by melting the LiBr/wax microspheres. This technique paves the way for realizing transient bioelectrical devices inspired by biological behavior, which have been well optimized by nature *via* evolution.

Received 20th March 2019
Accepted 29th April 2019

DOI: 10.1039/c9ra02147g

rsc.li/rsc-advances

1. Introduction

Transient electronic devices can be chemically and/or physically triggered by chemical etching,[1] humidity,[2] heat,[3] or light,[4] and they are applied in various fields, such as biomedical applications,[5–7] remote environmental sensors,[8] and multifunctional devices with temporal functional profiles. In nature, silkworm pupa become a juvenile moth in the cocoon during the larval stage, and the cocoon is camouflaged such that predators cannot see the interior. After the larval stage, the moth secretes cocoonase on one side of the cocoon to soften and break the cocoon. In this paper, we will fabricate transient dissolution electrical devices based on silk fibroin (SF) material inspired by the natural phenomenon of a silk cocoon protecting a silkworm pupa and a juvenile moth secreting an enzyme to dissolve silk sericin and break a silk cocoon. The devices can be destroyed by heat-sensitive microspheres in a controlled manner.

SF materials, medical materials approved by the US Food and Drug Administration (FDA), have been widely used in biomedical and tissue engineering applications due to their good *in vitro* and *in vivo* biocompatibility,[9–11] excellent mechanical properties,[12] and controllable biodegradation rate.[13] Recently, SF materials also emerged in the field of bioelectronics as a passive supporting materials.[14–16] For instance, the functional electric circuits can be attached onto the surface of flexible SF membranes by means of printing and thermal evaporation, *etc.*[17] Attributed to the great biocompatibility of SF membranes, these hybrid circuit/SF devices can be implanted into the human body while still maintaining circuit functionality.[18,19] Additionally, silk proteins can serve an electrical function in biodevices,[20,21] such as acting as the dielectric layer in organic field-effect transistors (OFETs)[7] and a storage layer in memristors.[22]

In this paper, we prepared thermal-triggered transient electronics by assembling heat-sensitive microspheres into SF conductive film, LED circuit on SF film, Ag/SF film/Pt/SF film memristor, respectively. Different from traditional electronic devices, our transient devices have transient behaviour. For regular applications, these devices maintain their full characteristics and functionalities to ensure reliable performance. However, upon heating these devices to a critical temperature, the protective wax shell melts and releases the encapsulated LiBr solution, which subsequently breaks the hydrogen bonds

[a]*Research Institution for Biomimetics and Soft Matter, Fujian Key Provincial Laboratory for Soft Functional Materials Research, College of Materials, Xiamen University, 422 Siming South Road, Xiamen, 361005, People's Republic of China. E-mail: linnaibo@xmu.edu.cn*

[b]*Department of Physics, National University of Singapore, 2 Science Drive 3, Singapore, 117542, Republic of Singapore*

† Electronic supplementary information (ESI) available: See DOI: 10.1039/c9ra02147g

between SF molecules and rapidly destroys the whole SF film. The associated electronic components will also degrade along with the SF film in a controllable manner (Fig. 1).

To the best of our knowledge, this study is the first to fabricate transient electronic devices inspired by the natural phenomenon, and the fabrication process has the following advantages: (i) no corrosive chemicals, such as strong acid, alkali, or organic solvents, are used; (ii) the process is simple and biologically friendly; and (iii) the process is a universally applicable strategy for destroying various biodevices on SF-based substrates.

2. Experimental section

2.1 Materials

Sodium carbonate anhydrous (analytically pure, Xilong Scientific Co., Ltd.), lithium bromide (99%, Shanghai Aladdin Biochemical Technology Co., Ltd.), lissamine rhodamine B (98%, Shanghai Aladdin Biochemical Technology Co., Ltd.), glycerol ($HOCH_2CHOHCH_2OH$, Xilong Scientific Co., Ltd.), biological glue (ELASTOSIL® E41), poly(vinyl alcohol) (PVA, M_w: 13 000–23 000 g mol^{-1}, 88% hydrolyzed, Shang Hai Yingjia Industrial Development Co., Ltd.), wax (C_nH_{2n+2}, mp 40 °C), deionized water, ultra-pure water, Span 80 (sorbitan monooleate, MACKLIN, $C_{24}H_{24}O_6$, 428.61 M_w), polyvinylpyrrolidone (molecular weight 1 300 000, Shanghai Aladdin Biochemical Technology Co., Ltd.), copper nitrate trihydrate (purity 99%, Beijing Yinuokai Technology Co., Ltd.), ethylene glycol (purity greater than 99%, Shanghai Aladdin Biochemical Technology Co., Ltd.), silver nitrate (analytically pure, Xilong Scientific Co., Ltd.), acetone (analytically pure, Sinopharm Chemical Reagent Co., Ltd.), ethanol (analytically pure, Sinopharm Chemical Reagent Co., Ltd.), borosilicate glass (SUTTER INSTRUMENT), SPI conductive silver paint (12 milliΩ per square, USA, SPI COMPANY), glass slides (microscope slides, China), square tubes (internal diameter: 1.0 mm, exterior diameter: 1.65 mm), in-line light-emitting diode (LED, Keyun Electronics), plastic needles (internal diameter: 1.30 mm, exterior diameter: 1.60 mm), and polytetrafluoroethylene tubes (internal diameter: 1.65 mm).

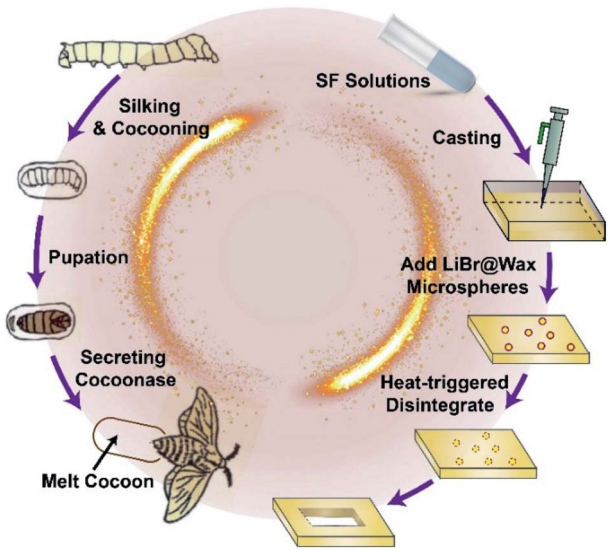

Fig. 1 Inspired by the natural phenomenon that a silk cocoon protecting silkworm pupa, and a juvenile silkworm moth secreting an enzyme to dissolve silk sericin and break a silk cocoon. Heat-triggerable transient electronics were assembled with wax microspheres containing LiBr solution. The LiBr solution can be released by melting the wax coating, leading to rapid electronic destruction.

2.2 Preparation of microcapsules

In this paper, the preparing process of the heat-sensitive microspheres with a 9.3 mol L^{-1} LiBr solution in wax shells is similar to that of the double emulsions based on microfluidic technology.[23–26] The capillary microfluidic device was assembled by coaxially aligning two cylindrical capillaries inside a square capillary, as shown in Fig. 2. The fluid of the inner phase was pumped through the first cylindrical capillary or injection tube, and the middle phase flowed through the interstices between the outer square capillary and the capillary through which the inner fluid was injected. The outer phase flowed into the square capillary from the opposite end. To keep the middle phase molten, the entire device was kept at 50 °C. The hydrodynamical flow of the outer phase focuses the inner and middle phases when they meet at the entrance of the second cylindrical capillary or collection tube. The molten middle phase (wax) is immiscible with both the inner and outer fluids, and double emulsions were formed inside the collection tube. The double emulsions were then quickly cooled below the melting temperature of the shell phase to form solid capsules. The encapsulated LiBr solution can be released on-demand by heating the capsules. Herein, the LiBr solution is selected due to its nontoxicity and high efficiency for dissolving SF. The continuous phase was a one-to-one weight ratio mixture of water and glycerol with 5 wt% PVA. The middle phase was wax with 6% surfactant (Span 80). The inner phase was a 9.3 mol L^{-1} LiBr solution with 0.06 wt% rhodamine B for visual observation. The flow rates of the outer, middle and inner phases were 25 000, 4000, and 4000 μL h^{-1}, respectively.

All fluids were pumped into the capillary microfluidic device using syringe pumps. We controlled the temperature of the molten phase by placing all syringe pumps into a 50 °C oven, which enabled temperature-controlled dispensal of the fluid with 1 °C precision.

2.3 Preparation of SF films

Bombyx mori cocoons were boiled in 0.02 M Na_2CO_3 for 30 min three times and rinsed with water. The degummed silk was

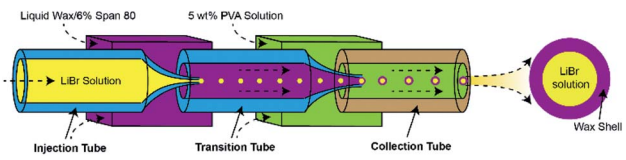

Fig. 2 Schematic illustration of the LiBr@Wax microspheres preparation process by glass capillary-based microfluidic devices.

dissolved in 9.3 mol L^{-1} aqueous LiBr at 60 °C for 4 h and then dialyzed with distilled water using dialysis cassettes for a couple of days to remove LiBr. After centrifugation and filtration to remove insoluble remnants, the resulting aqueous solutions were 6–10% (w/v) SF and preserved by storage at 5 °C. Then, 300 μL of SF solution with 20 wt% glycerin was dropped onto 2.5 × 2.5 cm glass slides and placed in an oven at 25 °C to dry and form a film.

2.4 Preparation of SF conductive film

A 100 μL aliquot of 4 mg mL^{-1} silver nanowires was dropped on 2.5 × 2.5 cm glass slides and dried in an oven at 60 °C. Then, 300 μL of SF solution with 20 wt% glycerin was applied dropwise to the slides, and the slides were placed in an oven at 25 °C to dry and form a film. The obtained film was torn off the slides, and silver nanowires were transferred to the free-standing SF film. The film was cut into 1 × 1 cm pieces, and the resistance of the film was measured to be approximately 20 ohms.

2.5 Fabrication of LED circuit

A layer of SF film is spin-coated on a glass substrate, and then Ag electric circuit (≈300 nm thick) for LED were deposited with e-beam evaporation with a high resolution stencil mask and conductive wires were attached with conductive silver epoxy.

2.6 Fabrication of SF memristor

SF solution was coated on glass slides and dried at 60 °C to form a SF film. A layer of platinum was deposited on the surface of the SF film, and then, SF was spun cast for 30 s at 1000 rpm to form a thin, 14 μm film. A silver electrode array was sputtered on the surface of a SF film through a mask plate. All the coated layers were peeled off the glass substrate to obtain a free-standing, flexible SF memristor.

2.7 Cytotoxicity assay

In order to test the cytotoxicity of the materials, the rMSC cells were seeded in 24-well plate with a density of 40 000 cells per well and incubated overnight at 37 °C. And then the materials were added into wells respectively and incubated with cells for 8 h at 37 °C. Then adding WST-1 to the culture medium of each sample and continue to incubate for 16 hours. To determine the cell viability, the absorbance near the wavelength of 570 nm was measured by a microplate reader (SpectraMax M2).

3. Results and discussion

Microfluidic technology was applied to synthesize our heat-sensitive microspheres, and a 9.3 mol L^{-1} LiBr solution was encapsulated in wax shells using glass capillary-based microfluidic devices (Fig. 2 and S1–S3†).[27,28] The resulting monodispersed water-in-oil-in-water double emulsions were characterized by optical microscopy. A core–shell structure was clearly observed, and the statistical results revealed an average diameter of 350 μm (Fig. 3). For visual observation, the LiBr solution was mixed with rhodamine B (0.5 wt%).

To quantify the dissolution ability of LiBr@Wax microspheres on SF films, a transient device with a sandwiched structure was designed. The top and bottom layers were two SF films with the same size of 1 × 1 cm and a thickness of 100 μm (Experimental section); the middle layer consisted of microspheres flatted on the SF films. After biological glue (ELASTOSIL® E41, Wacker) was applied to adhere the two films, a transient SF device was obtained.

The melting process of our device is not instant but transient, melting begins at several pores in the middle area of the device and is then followed by the collapse of the whole SF film. To study the influence of the microsphere content on the disintegration ability, we fabricated a series of transient SF devices incorporating varying microsphere quantities (*i.e.*, 40 wt%, 50 wt%, 60 wt%, 70 wt%, and 80 wt%, Fig. 4A). The degree of disintegration can be simply measured by calculating the portion of the dissolved area. To precisely calculate the areas of the SF films, the analytical software ImageJ was applied. The transient time is defined as the time at which the degree of disintegration reaches 20%.

When the transient SF devices were maintained at 60 °C for 7 min, the degree of disintegration increased from 7.8% to 45.3% as the mass fraction of the LiBr@Wax microspheres increased from 50 wt% to 80 wt% (Fig. 4A and B).

Obviously, the disintegration of the SF devices requires a critical concentration of microspheres. We noted that when the microsphere content decreased to 40 wt%, the SF devices did not show any dissolution, even after 70 min (Fig. S4†). When the mass fraction of microspheres was increased to 80 wt%, the devices were completely dissolved except for the area with biological glue, which indicated more LiBr solution was released from the wax microspheres (Fig. 4A). The correlation curve for the transient time and the microsphere content (Fig. 4B) indicates that as the microsphere content increases, the transient time decreases. A high content of microspheres will result in a very short transient time (2.25 min). In this article, we selected a microsphere mass fraction of 70 wt% for further investigation.

For a transient SF device with 70 wt% of LiBr@Wax microspheres, the degree of disintegration increases from 0% to 31.4% (Fig. 4C) from 1 to 9 min at 60 °C, and the transient time is 5.33 min. We also investigated the correlation between the degree of disintegration and the operation temperature and found that higher temperatures accelerated the disintegration process. For instance, after heating for 5 min, the degrees of disintegration are 0% and 32.8% at 40 °C and 80 °C, respectively

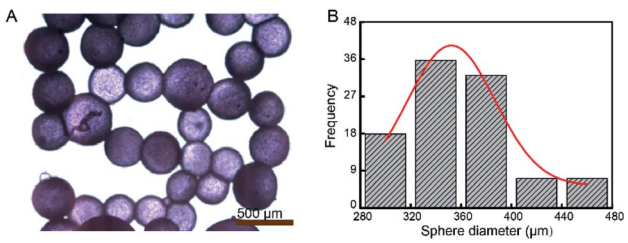

Fig. 3 (A) Optical microscopy imaging of the microspheres. (B) The size distribution of the LiBr@Wax microspheres.

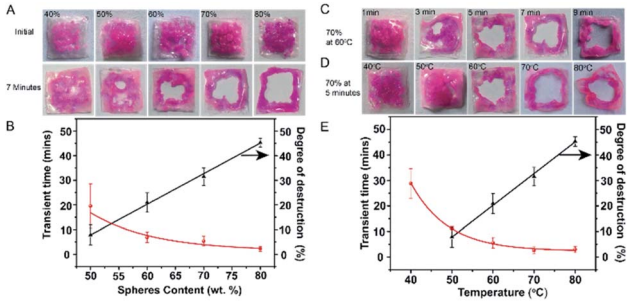

Fig. 4 (A) Images of SF films with different contents of LiBr/wax microspheres before heat triggering and after 7 min of heating. (B) Correlation between the microsphere contents in the SF film and transient time/the degree of destruction after 7 min of heating. (C) The dissolution process of a silk film with 70% LiBr@Wax microspheres at 60 °C. (D) Degradation of silk films with 70% LiBr@Wax microspheres at different temperatures after 5 min. (E) Effect of temperature on transient time and degree of destruction of silk films with 70% LiBr@Wax microspheres.

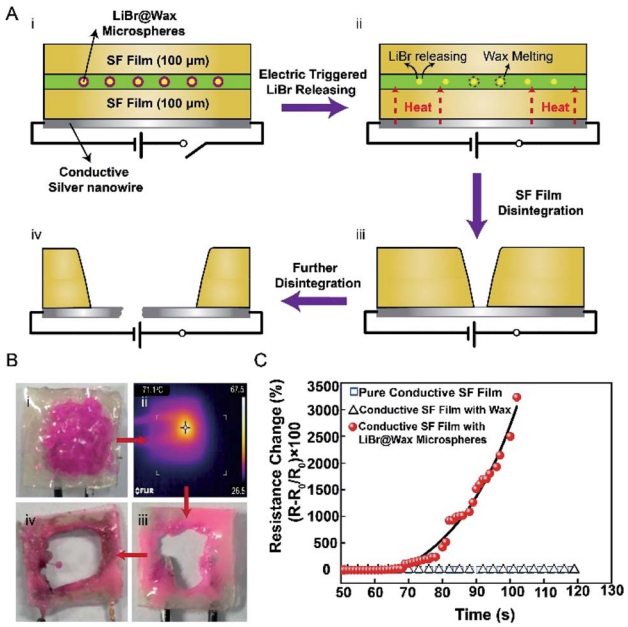

Fig. 5 (A) Schematics of the structure and operational principle of a transient device with a Ag nanowire resistor on a silk film substrate. (i) The Ag resistor on a silk film substrate coated with 70% LiBr@Wax microspheres. (ii) Heat-triggered disintegration of the device at 70 °C. (iii) Disintegration of the silk film substrate. (iv) Further disintegration. (B) Image of heat-triggered degradation of the device at 70 °C. (ii) Thermal infrared imaging of the transient device. (C) The resistance transient change of the device trigger by heat at 70 °C.

(Fig. 4D). The transient time increases from 28.8 s to 3 min as the temperature increases from 40 °C to 70 °C, and higher temperatures (*i.e.*, 80 °C) did not affect the transient time due to the fixed melting point of the wax shell (Fig. 4E).

Heat-triggered degradation was further demonstrated on a transient SF device with the same structure mentioned above except one side of the SF film substrate was coated with Ag nanowires (thickness *ca.* 300 nm, Fig. S6† and 5A). The resistance of the 1 × 1 cm flexible conducting films was measured to be approximately 20 ohms. Device failure (*i.e.*, transient time) was defined as a 500% increase in resistance to standardize our analysis. Prior to thermal triggering, the SF films coated by 70 wt% LiBr/wax microspheres showed a highly stable response (negligible resistance change) for one month at room temperature (Fig. S7†). Once the transient SF device was powered and heated by a digital meter at 2 V, the resistance of the monitored film quickly increased and caused resistor failure within 2 min (Fig. 5B and C). The thermal images showed that the temperature reached 70 °C in the center of the device. SF film degradation revealed the melting of the LiBr/wax microspheres released the LiBr solution, and the LiBr solution dissolved the SF protein and subsequently destroyed the Ag nanowires. In contrast, the resistance change in the device with a middle layer of pure wax was negligible under the same bias voltage of 2 V, and the SF film did not degrade (Fig. S8†).

Programmed degradation of selected electronic components can allow changes in the device geometry or direction of current flow in a circuit, altering or transforming the functionality of the electronic device. Previously reported transient systems that rely on the dissolution of components are difficult to design with selective or programmed transience.[15] Selective heat-triggered disintegration of an electronic device was achieved by selectively coating LiBr@Wax microspheres on a SF substrate. The device was composed of two LEDs connected in parallel with an Ag electrode. The Ag traces connected to the red LEDs were partially coated with LiBr/wax microspheres. The Ag trace to the blue LED was uncoated (Fig. 6A). Heat was applied to the circuit (70 °C) to activate the trigger, and the red LED dimmed as the Ag interconnection was destroyed by the LiBr solution in the coated area within approximately 5 min. After heating, only the blue LED continued to operate and was unaffected by the thermal treatment.

The memristor, the fourth fundamental electric element, was conceptually proposed by L. Chua in 1971 and created in a laboratory in late 2008; a memristor can mimic the behavior of neural synapses.[17] Base on the ability to retain data by "remembering" the amount of charge that has passed through them, *i.e.* resistive switching behaviour, the new memristor technology can store up to 128 discernible memory states per switch, which is almost four times higher than the traditional memory transistor.[29] The resistive switching behaviour is mostly attributed to the formation or rupture of nanoscale conductive filaments embedded in the insulating matrix. SF is among the most representative of proteins that have shown resistive switching effect,[30,31] and due to its advantageous properties, such as mechanical robustness, flexibility in thin-film form, optical transparency, and compatibility with aqueous processing, SF was selected as the functional material in our switching behaviour devices.

A SF-based memristor was fabricated, and LiBr/wax microspheres were placed on the surface of the SF substrate (Experimental section). Here, we employed a metal–insulator–metal structure to demonstrate a resistive memory device, in which Pt and Ag serve as inert and active electrodes, respectively (Fig. 6B).

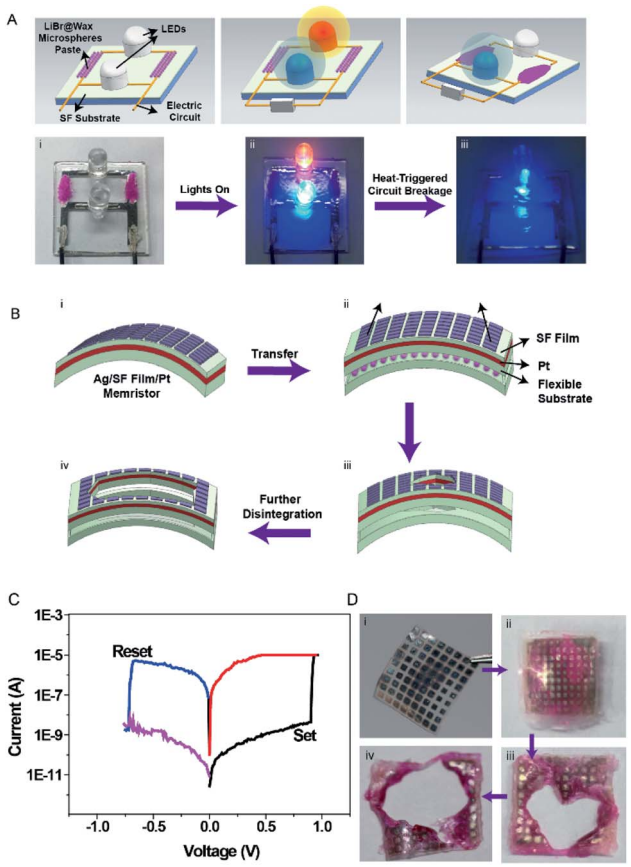

Fig. 6 (A) Multistage transition of LEDs achieved by selective microsphere coatings. The melting of LiBr/wax microspheres degrades the coated area at the desired temperature. (B) Illustration of transient dissolution of the silk-based memristor device. (i) The structure of the Ag/SF film/Pt memristor. (ii) Ag/SF film/Pt memristor on a flexible silk substrate with LiBr@Wax microspheres. (iii) Heat-triggered disintegration of the device at 70 °C. (iv) Further disintegration. (C) Typical current *versus* voltage (*I*/*V*) curves of the Ag/SF film/Pt memristor in voltage sweeping mode at ambient condition. (D) Images of the disintegration process of the Ag/SF film/Pt memristor.

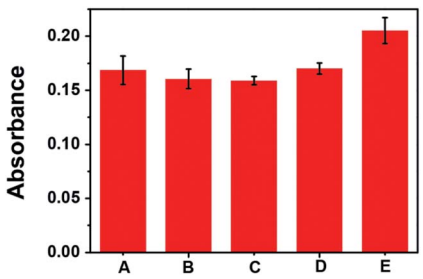

Fig. 7 The absorbance of each sample A–E.

Fig. 6Cshows typical *I*–*V* curves of the silk fibroin/Pt/silk fibroin/Ag devices with an area of 500 × 500 μm^2 structure under the voltage bias 0 → 1 → 0 → −1 → 0 V applied to Ag electrode, while Pt electrode was grounded. The as-fabricated device is in a high-resistance state. For positive bias sweep, the current maintains low under low electric field range. When the voltage reaches a certain value of 0.9 V (set voltage), the total current passes through the device increased abruptly, indicating high-to-low resistive switching (set process). A compliance current of 1 mA is set as the maximum current during set operation to prevent the device from breakdown. For the negative bias sweep, the initial state is a low-resistance state. When a certain negative voltage of −0.75 V (reset voltage) is reached, the resistance switches to a high-resistance state abruptly, indicating reset process. The *I*–*V* characteristic exhibits a typical bipolar resistive switching behavior.

After heat triggering at 70 °C, the memristor was mostly destroyed within 5 min, and complete disintegration of the device was achieved within 10 min (Fig. 6B and C).

The cytotoxicity of five samples were tested. Sample A: a transient device has a transient device with a sandwiched structure, a size of 1 × 1 cm SF film and a thickness of 100 μm as mentioned before consisted of 70% of LiBr@Wax microspheres. Sample B: Sample A was placed on a heating table to heat up to 70 °C, the microspheres were released and the SF was dissolved. Sample C, similar with Sample A except LiBr@Wax microspheres was replaced by the same weight wax. Sample D, similar with Sample A except it has no LiBr@Wax microspheres. Sample E, blank sample. From Fig. 7, all samples show no obvious distinguish. It means that the cytotoxicity of LiBr@Wax microspheres and SF materials is low.

4. Conclusions

These thermally transient bioelectrical devices that biomimic a SF moth breaking out of its cocoon can isolate and release a degradation agent (the LiBr solution), and the transient response is fast and adjustable. The content of LiBr@Wax microspheres in the SF and the temperature have a significant impact on the transient time. The transient dissolution of SF-based Ag-nanowire resistance circuit lines and memristors indicates that this approach is feasible and effective. This approach provides a simple and versatile platform for not only controllable dissolution of SF matrix bioelectronic devices but also the disintegration of other biomaterial devices, such as those created with cellulose, protein or artificial polymer, which will play important roles in biomedicine (such as sensors[32,33]), information storage (such as memristors[34]) and other fields.

Conflicts of interest

There are no conflicts to declare.

Acknowledgements

The work was supported by the National Natural Science Foundation of China (Grant Nos. 51773171, 21705135), the Fujian Provincial Department of Science and Technology (Grant No. 2017J06019), the 111 Project (Grant No. B16029), the China Postdoctoral Science Foundation (Grant No. 2017M612133), the Fundamental Research Funds for the Central Universities (Grant No. 20720170019) and NUS tear 1 funding (WBS: R-144-

000-367-112). The primary affiliation of X.-Y. Liu is the Department of Physics, National University of Singapore.

Notes and references

1 C. H. Lee, S.-K. Kang, G. A. Salvatore, Y. Ma, B. H. Kim, Y. Jiang, J. S. Kim, L. Yan, D. S. Wie, A. Banks, S. J. Oh, X. Feng, Y. Huang, G. Troester and J. A. Rogers, *Adv. Funct. Mater.*, 2015, **25**, 5100–5106.
2 S. H. Jin, S. K. Kang, I. T. Cho, S. Y. Han, H. U. Chung, D. J. Lee, J. Shin, G. W. Baek, T. I. Kim, J. H. Lee and J. A. Rogers, *ACS Appl. Mater. Interfaces*, 2015, **7**, 8268–8274.
3 C. W. Park, S.-K. Kang, H. L. Hernandez, J. A. Kaitz, D. S. Wie, J. Shin, O. P. Lee, N. R. Sottos, J. S. Moore, J. A. Rogers and S. R. White, *Adv. Mater.*, 2015, **27**, 3783–3788.
4 H. L. Hernandez, S. K. Kang, O. P. Lee, S. W. Hwang, J. A. Kaitz, B. Inci, C. W. Park, S. Chung, N. R. Sottos, J. S. Moore, J. A. Rogers and S. R. White, *Adv. Mater.*, 2014, **26**, 7637–7642.
5 S.-W. Hwang, D.-H. Kim, H. Tao, T.-i. Kim, S. Kim, K. J. Yu, B. Panilaitis, J.-W. Jeong, J.-K. Song, F. G. Omenetto and J. A. Rogers, *Adv. Funct. Mater.*, 2013, **23**, 4087–4093.
6 C. J. Bettinger and Z. Bao, *Adv. Mater.*, 2010, **22**, 651–655.
7 M. Irimia-Vladu, P. A. Troshin, M. Reisinger, L. Shmygleva, Y. Kanbur, G. Schwabegger, M. Bodea, R. Schwödiauer, A. Mumyatov, J. W. Fergus, V. F. Razumov, H. Sitter, N. S. Sariciftci and S. Bauer, *Adv. Funct. Mater.*, 2010, **20**, 4069–4076.
8 S. W. Hwang, C. H. Lee, H. Cheng, J. W. Jeong, S. K. Kang, J. H. Kim, J. Shin, J. Yang, Z. Liu, G. A. Ameer, Y. Huang and J. A. Rogers, *Nano Lett.*, 2015, **15**, 2801–2808.
9 Z. Z. Shao and F. Vollrath, *Nature*, 2002, **418**, 741.
10 C. Vepari and D. L. Kaplan, *Prog. Polym. Sci.*, 2007, **32**, 991–1007.
11 F. G. Omenetto and D. L. Kaplan, *Science*, 2010, **329**, 528–531.
12 S. Keten, Z. Xu, B. Ihle and M. J. Buehler, *Nat. Mater.*, 2010, **9**, 359–367.
13 Y. Wang, D. D. Rudym, A. Walsh, L. Abrahamsen, H. J. Kim, H. S. Kim, C. Kirker-Head and D. L. Kaplan, *Biomaterials*, 2008, **29**, 3415–3428.
14 S. Ling, C. Li, K. Jin, D. L. Kaplan and M. J. Buehler, *Adv. Mater.*, 2016, **28**, 7783–7790.
15 S. W. Hwang, S. K. Kang, X. Huang, M. A. Brenckle, F. G. Omenetto and J. A. Rogers, *Adv. Mater.*, 2015, **27**, 47–52.
16 M. A. Brenckle, H. Cheng, S. Hwang, H. Tao, M. Paquette, D. L. Kaplan, J. A. Rogers, Y. Huang and F. G. Omenetto, *ACS Appl. Mater. Interfaces*, 2015, **7**, 19870–19875.
17 H. Wang, B. Zhu, H. Wang, X. Ma, Y. Hao and X. Chen, *Small*, 2016, **12**, 3360–3365.
18 D.-H. Kim, J. Viventi, J. J. Amsden, J. Xiao, L. Vigeland, Y.-S. Kim, J. A. Blanco, B. Panilaitis, E. S. Frechette, D. Contreras, D. L. Kaplan, F. G. Omenetto, Y. Huang, K.-C. Hwang, M. R. Zakin, B. Litt and J. A. Rogers, *Nat. Mater.*, 2010, **9**, 511–517.
19 C. H. Wang, C. Y. Hsieh and J. C. Hwang, *Adv. Mater.*, 2011, **23**, 1630–1634.
20 C. Wang, X. Li, E. Gao, M. Jian, K. Xia, Q. Wang, Z. Xu, T. Ren and Y. Zhang, *Adv. Mater.*, 2016, **28**, 6640–6648.
21 B. Zhu, H. Wang, W. R. Leow, Y. Cai, X. J. Loh, M. Y. Han and X. Chen, *Adv. Mater.*, 2016, **28**, 4250–4265.
22 Y. S. Yun, S. Y. Cho, J. Shim, B. H. Kim, S. J. Chang, S. J. Baek, Y. S. Huh, Y. Tak, Y. W. Park, S. Park and H. J. Jin, *Adv. Mater.*, 2013, **25**, 1993–1998.
23 R. Gao, N. Choi, S. I. Chang, E. K. Lee and J. Choo, *Nanoscale*, 2014, **6**, 8781–8786.
24 A. Yashina, I. Lignos, S. Stavrakis, J. Choo and A. J. deMello, *J. Mater. Chem. C*, 2016, **4**, 6401–6408.
25 T. Yang, J. Choo, S. Stavrakis and A. de Mello, *Chemistry*, 2018, **24**, 12078–12083.
26 J. Jeon, N. Choi, H. Chen, J. I. Moon, L. Chen and J. Choo, *Lab Chip*, 2019, **19**, 674–681.
27 M. Windbergs, Y. Zhao, J. Heyman and D. A. Weitz, *J. Am. Chem. Soc.*, 2013, **135**, 7933–7937.
28 W. Wang, T. Luo, X.-J. Ju, R. Xie, L. Liu and L.-Y. Chu, *Int. J. Nonlinear Sci. Numer. Simul.*, 2012, **13**, 325–332.
29 K. H. Kim, S. Gaba, D. Wheeler, J. M. Cruz-Albrecht, T. Hussain, N. Srinivasa and W. Lu, *Nano Lett.*, 2012, **12**, 389–395.
30 H. Wang, F. Meng, Y. Cai, L. Zheng, Y. Li, Y. Liu, Y. Jiang, X. Wang and X. Chen, *Adv. Mater.*, 2013, **25**, 5498–5503.
31 M. K. Hota, M. K. Bera, B. Kundu, S. C. Kundu and C. K. Maiti, *Adv. Funct. Mater.*, 2012, **22**, 4493–4499.
32 S. W. Hwang, H. Tao, D. H. Kim, H. Cheng, J. K. Song, E. Rill, M. A. Brenckle, B. Panilaitis, S. M. Won, Y. S. Kim, Y. M. Song, K. J. Yu, A. Ameen, R. Li, Y. Su, M. Yang, D. L. Kaplan, M. R. Zakin, M. J. Slepian, Y. Huang, F. G. Omenetto and J. A. Rogers, *Science*, 2012, **337**, 1640–1644.
33 M. S. Mannoor, H. Tao, J. D. Clayton, A. Sengupta, D. L. Kaplan, R. R. Naik, N. Verma, F. G. Omenetto and M. C. McAlpine, *Nat. Commun.*, 2012, **3**, 763.
34 H. Wang, Y. Du, Y. Li, B. Zhu, W. R. Leow, Y. Li, J. Pan, T. Wu and X. Chen, *Adv. Funct. Mater.*, 2015, **25**, 3825–3831.